

KINEMATIC PROPERTIES OF YOUNG SUBSYSTEMS AND THE ROTATION CURVE OF OUR GALAXY

M.V. Zabolotskikh, A.S. Rastorguev, A.K. Dambis

Sternberg Astronomical Institute
119992, Universitetskij pr., 13, Moscow, Russia
E-mail: zabolot@sai.msu.ru

Abstract

The maximum-likelihood analysis is applied to space velocities of 113 classical Cepheids with periods longer than 9 days, 89 young open clusters with ages less than 40 Myr, 102 blue supergiants, 200 HII-regions and 150 HI radial velocities. We used the distance scales of objects balanced by the statistical-parallax technique. The kinematic properties of young subsystems have been derived (solar motion components, velocity-ellipsoid axes). The rotation curve is constructed from radial velocities of all objects on the galactocentric distances 2-14 kpc for short ($R_0 = 7.5$ kpc) and long ($R_0 = 8.5$ kpc) distance scale.

KEYWORDS: *Galaxy: kinematics, rotation curve, open clusters, Cepheids, blue supergiants, HI, HII*

1. Introduction

The parameters of the Galactic rotation curve were determined by many authors, but it should be pointed out that these parameters depend first on the correctness of the adopted distance scale of objects under study. Objects with known distances – classical Cepheids, open star clusters (OSC), and OB-associations – allow the rotation curve to be determined only out to heliocentric distances of 4-5 kpc, whereas HI and HII kinematic data allow constructing the rotation curve over a wider interval of galactocentric distances. The main problem of using the hydrogen data is that the distances of giant molecular clouds (GMC) and, consequently, those of HII-regions, are determined from their single hot exciting stars whose distance scale is prone to random and systematic errors. Therefore, our goal is to refine the distance scales of young subsystems and to construct the rotational curve of our Galaxy.

2. Observational Data

Our sample included 89 young OSC with $\log T < 7.6$ and heliocentric distances determined by Dambis (1999) by fitting Kholopov's (1980) ZAMS with allowance for evolutionary deviations based on Geneva-group isochrones (Maeder and Meynet 1991). The radial velocities of cluster members were determined by Glushkova based on published data and can be found in the paper by Rastorguev et al. (1999). The proper motions of clusters were computed from those of their member stars found in the HIPPARCOS catalog (Baumgardt et al. 2000).

We also used 113 classical Cepheids with periods $P > 9^d$ and heliocentric distances computed using the fundamental-mode period-luminosity relation of Berdnikov et al. (1996): $\langle M_K \rangle_I = -5.46^m - 3.52^m \log P$ in accordance with the procedure described therein. An earlier statistical-parallax analysis (Rastorguev et al. 1999) showed that the sample of Cepheids with shorter periods is not homogeneous in terms of pulsation mode and may be contaminated by first-overtone pulsators. We used published Cepheid radial velocities and HIPPARCOS proper motions. Young OSC and long-period Cepheids make up a kinematically homogeneous reference sample consisting of 176 and 142 objects with radial velocities and proper motions, respectively, including 124 objects with space velocities.

We performed a separate analysis of a blue supergiant sample consisting of 102 stars with heliocentric distances tied to the OSC distance scale (Dambis 1990). The proper motions of supergiants adopted from the HIPPARCOS catalog, and radial velocities from the catalogs of Barbier-Brossat and Figon (2000) and WEB (Dufhot et al. 1995).

Brand and Blitz (1993) published the distances and radial velocities for a total of 206 HII-regions. We selected 203 of these objects with spectroscopic or photometric distances inferred from their exciting stars. The radial velocities of HII-regions were determined from the CO (2.6-mm) radio lines of their associated molecular clouds. We did not include three HII-regions in the final list because of their large residual velocities relative to the provisional rotation-curve solution. The catalog mentioned above also gives standard errors of individual distances and line-of-sight velocities.

We adopted 150 tangent-point radial velocities of HI clouds from Fich et al. (1989). Note that published HI and HII radial velocities are traditionally corrected for the solar motion relative to the standard apex assumed to coincide with the local standard of rest (LSR), and therefore we first converted them into heliocentric radial velocities.

3. Method of Analysis

We used the techniques of maximum-likelihood and statistical parallax (including its simplified version) to compute the kinematic parameters and refine the distance scales involved. See Murray (1983) for a description of the principal ideas of the statistical-parallax method used in this paper. The tangential velocity of a star is computed from its proper motion and distance and therefore depends on the adopted distance scale, whereas radial velocities are distance independent. The distance scale factor is defined as $p = r_o/r_t$, where r_o is the adopted distance and r_t is the true distance. The gist of the method consists of reconciling the fields of radial and tangential velocities in terms of some model of the field of systematic motions and ellipsoidal distribution of residual velocities.

The residual velocity of a star can be written in the following form: $\Delta\mathbf{V} = \mathbf{V}_{obs} - \mathbf{V}_{sun} - \mathbf{V}_{rot}$, where \mathbf{V}_{obs} is the observed space velocity; \mathbf{V}_{sun} is the mean heliocentric velocity of the sample studied; \mathbf{V}_{rot} is the contribution of Galactic differential rotation. Residual space velocities are usually assumed to have a three-dimensional normal distribution: $f(\Delta\mathbf{V}) = (2\pi)^{-3/2} |L_{obs}|^{-1/2} \{-0.5\Delta\mathbf{V}^T \times L_{obs}^{-1} \times \Delta\mathbf{V}\}$, where the matrix of covariance L_{obs} contains the ellipsoidal velocity distribution, errors of distances, radial velocities and proper motion and influence of errors of distances on the systematic velocities. We inferred the unknown parameters by using the maximum-likelihood method or in other words by minimizing the function $LF = -\sum_{i=1}^N \ln f(\Delta\mathbf{V})$. To compute the parameter errors we used the method proposed by Hawley et al. (1986).

The simplified version of the statistical-parallax technique (as used, e.g., by Feast et al. 1998) based on reconciling the kinematic parameters inferred separately from radial velocities and proper motions. Thus it is well known that Oort's constant A inferred from proper motions is much less sensitive to the adopted distance scale than is the value of the same constant inferred from radial velocities. This allows not only the kinematic parameters to be determined but also the distance scale of objects under study to be refined. When refining the distance scale by reconciling the values of Oort's constant A we set $p = 1$.

4. Results and Discussion

First, we applied the maximum-likelihood method to our sample of Cepheids and OSC. Because the galactocentric distance of Sun R_0 and the distance scale

are correlated with each other, we performed our computations with two most commonly adopted values – $R_0 = 7.5$ and 8.5 kpc. We determined the angular velocity of galactic rotation from space velocities of Cepheids and OSC and then used it to construct the Galactic rotation curve based on the radial velocities of all objects considered. The dispersion of the inferred absolute magnitude is equal to $\sigma_M = 0.15^m$ for sample of Cepheids and OSC and $\sigma_M = 0.38^m$ for sample of blue supergiants. It should be noted that the study of the kinematics and space distribution in the disk of other galaxies showed the exponential decrease of surface brightness and velocity dispersion with galactocentric distance (Bottema 1993). But the real accuracy of the computed rotational curve allows us to get rid of this effect.

Table 1 lists the distance scale factors for our samples estimated by the statistical-parallax technique and its simplified version. We analyzed the problem of systematic differences between the distance scale factors given by this two methods. One hundred numerical simulations have shown that the distance scale factor is on the average equal to 1 from both methods and p_1 and p_2 are correlated with each other. We cannot unambiguously choose between the two approaches to the distance scale refinement. It is logical to associate the short and long distance scales with $R_0 = 7.5$ and $R_0 = 8.5$ kpc. In other words $p = 0.96 \rightarrow R_0 = 7.5$ kpc and $p = 0.84 \rightarrow R_0 = 8.5$ kpc for Cepheids+OSC sample and $p = 1.09 \rightarrow R_0 = 7.5$ kpc and $p = 0.97 \rightarrow R_0 = 8.5$ kpc for the blue supergiants sample.

Table 1. Distance scale factors estimated by the statistical-parallax technique (p_1) and by simplified version (p_2).

R_0 , kpc	p_1 ,	p_2 ,	p_1 ,	p_2 ,
	Cepheids+OSC		Supergiants	
7.5	0.86	0.96	1.09	0.97
8.5	0.84	0.97	1.09	0.97
errors	± 0.05	± 0.09	± 0.08	± 0.16

The only way to match the distance scales of HII and stars is to compare the first derivatives of angular velocities inferred from radial and space velocities for gas and stars, respectively. In the result $p = 0.95$ for $R_0 = 7.5$ kpc and $p = 0.90$ for $R_0 = 8.5$ kpc. The good agreement between mean heliocentric velocity components of different young-object samples allows us to construct the rotation curve over a sufficiently wide interval of galactocentric distances, 2 – 14 kpc, using radial velocities of both stars and gas (see Fig. 1, 2). The resulting local centroid velocity and Oort’s constant A

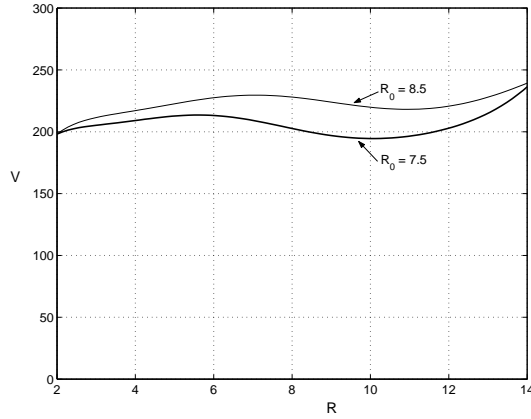


Figure 1: Galactic rotation curve $V(R)$ for the short ($R_0 = 7.5$ kpc) and long ($R_0 = 8.5$ kpc) distance scales

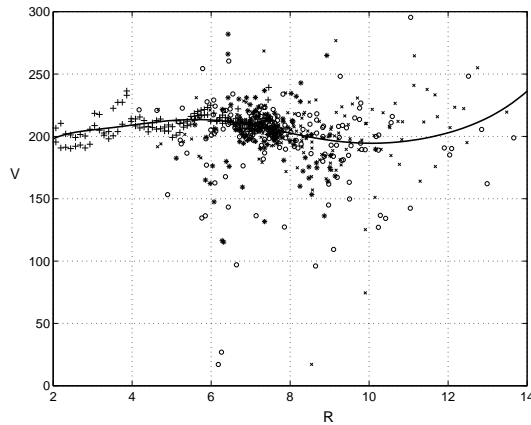


Figure 2: Galactic rotation curve $V(R)$ for the short distance scale ($R_0 = 7.5$ kpc) with young-object data points ("+" - HI, "x" - HII, "o" - Cepheids+OC, "*" - blue supergiants)

are equal to $V(R_0) = (206 \pm 10) \text{ km s}^{-1}$, $A = (17.1 \pm 0.5) \text{ km s}^{-1} \text{ kpc}^{-1}$ and $V(R_0) = (226 \pm 12) \text{ km s}^{-1}$, $A = (15.4 \pm 0.6) \text{ km s}^{-1} \text{ kpc}^{-1}$ for the short and long distance scale, respectively. We computed the velocity ellipsoid axes separately for Cepheids and OSC, supergiants and gas (see Table 2). We see that the axial ratio of the Cepheids and OSC velocity ellipsoid obeys closely to the Lindblad formula, whereas for the gas $\sigma_u \approx \sigma_v$.

Table 2. Heliocentric velocity components and velocity ellipsoid axes for the young object sample (* - fixing parameters).

	$\sigma_u,$ kms ⁻¹	$\sigma_v,$ kms ⁻¹	$\sigma_w^*,$ kms ⁻¹	$u_0,$ kms ⁻¹	$v_0,$ kms ⁻¹	$w_0^*,$ kms ⁻¹
Cepheids+OSC	13.30	7.59	7.55	-9.17	-12.98	-7.25
errors	±1.79	±0.41	—			
Supergiants	14.17	10.00	5.13			
errors	±0.51	±2.12	—			
HII	6.71	7.19	5.0			
errors	±0.60	0.93	—			
HI	6.60	6.05	5.0			
errors	—	±0.34	—	±0.48	±0.78	—

Acknowledgements

The work was supported by the Russian Foundation for Basic Research (grants nos. 01-02-06012, 00-02-17804, 99-02-17842, 01-02-16086, 02-02-16677, and 02-02-06593) and the Council for the Support of Leading Scientific Schools (grant no. 00-15-96627).

References

- Barbier-Brossat, M., Figon, P., 2000, A&AS 142, 217
Baumgardt, H., Dettbarn, C., Wielen, R., 2000, A&AS 146, 251
Berdnikov, L.N., Vozyakova, O.V., Dambis, A.K., 1996, Astron. Lett. 22, 838
Bottema, R., 1993, A&A 275, 16
Brand J., Blitz, L., 1993, A&A 275, 67
Dambis, A.K., 1990, Sov. Astron. Lett. 16, 224
Dambis, A.K., 1999, Astron. Lett. 25, 7
Duflot, M., Figon, P., Meyssonier, N., 1995, A&AS 114, 269
Feast, M., Pont, F., Whitelock, P., 1998, MNRAS 298, L43
Fich, M., Blitz, L., Stark, A.A., 1989, ApJ 342, 272
Hawley, S.L., Jeffreys, W.H., Barnes, III, T.J., L. Wan, 1986, ApJ 302, 626
Kholopov, P.N., 1980, Sov. Astron. 24, 7
Maeder F., Meynet, G., 1991, A&AS 89, 451
Murray, C.A., 1983, Vectorial Astrometry (A. Hilger, Bristol)
Rastorguev, A.S., Glushkova, E.V., Dambis, A.K., Zabolotskikh, M.V., 1999, Astron. Lett. 25, 595
The HIPPARCOS and TYCHO Catalogues, European Space Agency, 1997, ESA SP-1200